Observation of the multifractal spectrum in the heliosphere and the heliosheath by Voyager 1 and 2

W. M. Macek,[1,2,3] A. Wawrzaszek,[1] and V. Carbone[4]

Received 13 July 2012; revised 17 September 2012; accepted 6 October 2012; published 4 December 2012.

[1] We present first results of the multifractal scaling of the fluctuations of the interplanetary magnetic field strength as measured onboard Voyager 2 in the very distant heliosphere and even in the heliosheath. More specifically, the spectra observed by Voyager 2 in a wide range of heliospheric distances from 6 to 90 astronomical units (AU) are compared with those of Voyager 1 already analyzed between 7 and 107 AU. We focus on the singularity multifractal spectrum before and after crossing the termination heliospheric shock by Voyager 1 at 94 AU and Voyager 2 at 84 AU from the Sun. It is worth noting that the spectrum is prevalently right-skewed inside the whole heliosphere. Moreover, we have observed a change of the asymmetry of the spectrum at the termination shock, where the spectrum changes from (left-) right-skewed in the very distant heliosphere to the (right-) left-skewed or possibly symmetric spectrum in the heliosheath. We confirm that the degree of multifractality falls steadily with the distance from the Sun. In addition, the multifractal structure is apparently modulated by the solar activity, with a time shift of several years, corresponding to a distance of about 10 AU, resulting from the evolution of the whole heliosphere. Hence this basic result also brings significant additional support to some earlier claims suggesting that the solar wind termination shock is asymmetric.

Citation: Macek, W. M., A. Wawrzaszek, and V. Carbone (2012), Observation of the multifractal spectrum in the heliosphere and the heliosheath by Voyager 1 and 2, *J. Geophys. Res.*, *117*, A12101, doi:10.1029/2012JA018129.

1. Introduction

[2] The general aim of the present paper is to report on the new developments in systems exhibiting turbulent behavior by using multifractals, with application to phenomenological approach to this complex issue. Namely, following the idea of *Kolmogorov* [1941] and *Kraichnan* [1965], various multifractal models of turbulence have been developed [*Meneveau and Sreenivasan*, 1987; *Carbone*, 1993; *Frisch*, 1995].

[3] In order to look at the multifractal scaling of solar wind turbulence we have developed a generalized two-scale weighted Cantor set model [*Macek*, 2007; *Macek and Szczepaniak*, 2008]. This model has allowed us to obtain the spectrum of generalized dimensions and the multifractal singularity spectrum, which depend on one probability measure parameter and two other scaling model parameters. Namely, by using the partition technique, we have extensively studied the inhomogeneity of the rate of the transfer of the energy flux between cascading eddies. In this way, we have revealed a multifractal and intermittent behavior of solar wind turbulence [*Bruno and Carbone*, 2005]. In particular, we have investigated in detail fluctuations of the velocity of the flow of the solar wind, as measured in the inner heliosphere by Helios [*Macek and Szczepaniak*, 2008], Advanced Composition Explorer (ACE) [*Szczepaniak and Macek*, 2008], Voyager in the outer heliosphere [*Macek and Wawrzaszek*, 2009], and Ulysses observations at high heliospheric latitudes [*Wawrzaszek and Macek*, 2010].

[4] It is known that fluctuations of the solar magnetic fields also exhibit multifractal scaling laws. Namely, the multifractal structure has been investigated using magnetic field data measured in situ by Voyager in the outer heliosphere up to large distances from the Sun [*Burlaga*, 1991, 1995, 2001, 2004] and also in the heliosheath [*Burlaga and Ness*, 2010; *Burlaga et al.*, 2005, 2006]. In particular, the results of the generalized dimensions and the multifractal spectrum obtained by using the Voyager 1 data of the magnetic field strength have been presented at distances of 83.4–85.9 AU from the Sun, i.e., before the termination shock crossing [*Burlaga*, 2004], and in the heliosheath at 94.2–97.2 AU [*Burlaga et al.*, 2006] and 108.5–112.1 AU [*Burlaga and Ness*, 2010], correspondingly. We have also examined the question of scaling properties of intermittent solar wind magnetic turbulence looking at Voyager 1 data and using our

[1]Space Research Centre, Polish Academy of Sciences, Warsaw, Poland.
[2]Faculty of Mathematics and Natural Sciences, Cardinal Stefan Wyszyński University, Warsaw, Poland.
[3]Temporarily at NASA Goddard Space Flight Center, Greenbelt, Maryland, USA.
[4]Dipartimento di Fisica, Università della Calabria, Rende-Cosenza, Italy.

Corresponding author: W. M. Macek, Space Research Centre, Polish Academy of Sciences, Bartycka 18 A, 00-716 Warszawa, Poland. (macek@cbk.waw.pl)

0148-0227/12/2012JA018129

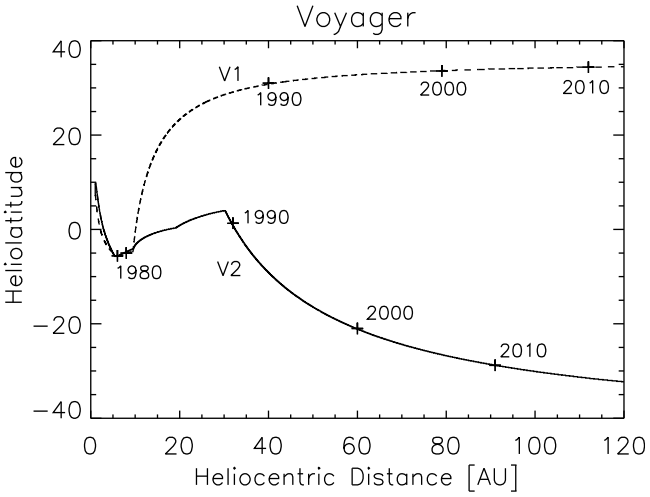

Figure 1. The heliospheric distances from the Sun and the heliographic latitudes during each year of the Voyager mission. Voyager 1 (dashed line) and 2 (continuous line) spacecraft are located above and below the solar equatorial plane, respectively [cf., e.g., *Richardson et al.*, 2004].

weighted two-scale Cantor set model at a wide range of the heliospheric distances [*Macek et al.*, 2011].

[5] Admittedly, variations of the magnetic field strength observed by Voyager 2 have also been analyzed including those prior and after crossing the termination shock up to distances of ~90 AU in 2009 (from 2007.7 to 2009.4), see [*Burlaga et al.*, 2008, 2009, 2010]. However, the multifractal spectrum using Voyager 2 data has only been analyzed at 25 AU by *Burlaga* [1991], but in a more distant heliosphere and especially near the termination shock this multifractal analysis is still missing.

[6] Therefore, the aim of our present study, which is a substantial extension of the previous letter [*Macek et al.*, 2011], is to investigate the multifractal scaling for both Voyager 1 and 2 data that will allow us to infer new information about the multifractal structure of the heliospheric magnetic fields in the northern and southern hemisphere, including the correlation with the solar cycle. In particular, we show that multifractal structure is modulated by the solar activity with some time delay and confirm that the degree of multifractality is also decreasing with distance: before shock crossing is greater than that in the heliosheath. Moreover, we demonstrate that the multifractal spectrum is asymmetric before shock crossing, in contrast to the nearly symmetric spectrum observed in the heliosheath; the solar wind in the outer heliosphere may exhibit strong asymmetric scaling, where the spectrum is prevalently right-skewed. The obtained delay between Voyager 1 and 2 can certainly be correlated with the evolution of the heliosphere, providing an additional support to some earlier independent claims that the solar wind termination shock itself is possibly asymmetric [*Stone et al.*, 2008].

2. Data Analysis

[7] Voyager 1 crossed the termination heliospheric shock, which separates the Solar System plasma from the surrounding heliosheath, with the subsonic solar wind, on 16 December 2004 at heliocentric distances of 94 AU (at present its distance to the Sun is about 122 AU approaching the heliopause). Please note that (using the pressure balance) the distance to the nose of the heliopause has been estimated to be ~120 AU [*Macek*, 1998]. Later, in 2007 also Voyager 2 crossed the termination shock at least five times at distances of 84 AU (now is at 100 AU). The data have revealed a complex, rippled, quasi-perpendicular supercritical magnetohydrodynamic shock of moderate strength with a reformation of the shock on a scale of a few hours, suggesting the importance of ionized interstellar atoms (so-called 'pickup' protons) at the shock structure [*Burlaga et al.*, 2008].

[8] The main objective of this study is to test the multifractal scaling of the interplanetary magnetic field strength for the wealth of data provided by Voyager mission, exploring various regions of space magnetized plasmas. Therefore, we also analyze time series of the magnetic field fluctuations measured by Voyager 2 at a wide range of distances before the termination shock crossing (during years 1980–2006), namely between ~5 and ~80 AU from the Sun, and subsequently (2008–2009) at 85–90 AU, i.e., in the heliosheath. This will allow us to compare the new results with those for Voyager 1 as already discussed by *Macek et al.* [2011]. The heliospheric distances from the Sun and the heliographic latitudes during each year of the Voyager mission are given in Figure 1 [cf., e.g., *Richardson et al.*, 2004]. We see that Voyager 1 and 2 spacecraft are located above and below the solar equatorial plane, respectively.

3. Multifractal Model

[9] The multifractals are described by an infinite number of the generalized dimensions, D_q, and by the multifractal spectrum $f(\alpha)$ [e.g., *Ott*, 1993]. The generalized dimensions D_q are calculated as a function of a continuous index q [*Grassberger and Procaccia*, 1983; *Hentschel and Procaccia*, 1983; *Halsey et al.*, 1986]. In our case high positive values of q emphasize regions of intense magnetic fluctuations larger than the average, while negative values of q accentuate fluctuations lower than the average [*Burlaga*, 1995].

[10] Alternatively, we can describe intermittent turbulence by using the singularity spectrum $f(\alpha)$ as a function of a singularity strength α, which quantifies multifractality of a given system. This function sketched in Figure 2 describes singularities occurring in considered probability measure, allowing a more clear theoretical interpretation by comparing the experimental results with those obtained from phenomenological models of turbulence [*Halsey et al.*, 1986; *Ott*, 1993; *Wawrzaszek and Macek*, 2010].

3.1. Structure of Interplanetary Magnetic Fields

[11] Following *Burlaga* [1995], let us take a stationary magnetic field $B(t)$ in the heliosphere. We can decompose this signal into time intervals of size Δt corresponding to the spatial scales $l = v_{sw}\Delta t$, where v_{sw} is the solar wind speed. Then to each time interval one can associate a magnetic flux past the cross-section perpendicular to the plane during that time. In every considered year we use a discrete time series of daily averages, which is normalized so that we have $\langle B(t)\rangle = \frac{1}{N}\sum_{i=1}^{N} B(t_i) = 1$, where $i = 1, \ldots, N = 2^n$ (taking $n = 8$). Next, given this (normalized) time series $B(t_i)$, to

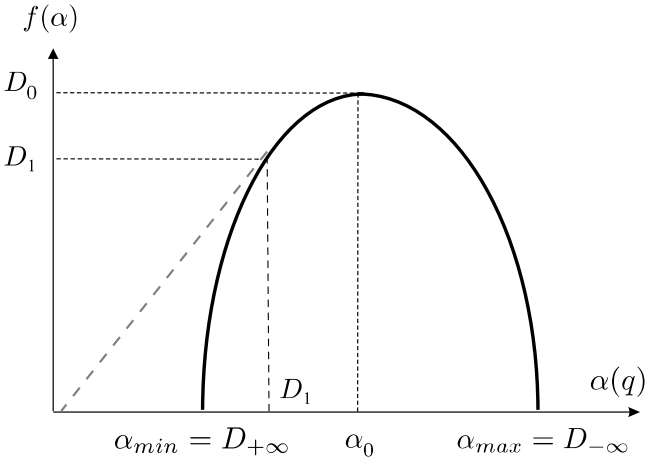

Figure 2. The singularity multifractal spectrum $f(\alpha)$ versus the singularity strength α with some general properties: (1) the maximum value of $f(\alpha)$ is D_0; (2) $f(D_1) = D_1$; and (3) the line joining the origin to the point on the $f(\alpha)$ curve where $\alpha = D_1$ is tangent to the curve, as taken from *Ott* [1993].

each interval of temporal scale Δt (using $\Delta t = 2^k$, with $k = 0, 1, \ldots, n$) we associate some probability measure

$$p(x_j, l) \equiv \frac{1}{N} \sum_{i=1+(j-1)\Delta t}^{j\Delta t} B(t_i) = p_j(l), \tag{1}$$

where $j = 2^{n-k}$, i.e., calculated by using the successive average values $\langle B(t_i, \Delta t)\rangle$ of $B(t_i)$ between t_i and $t_i + \Delta t$ [*Burlaga et al.*, 2006].

3.2. Multifractal Formalism

[12] Using the measure defined in Subsection 3.1 we can construct both functions D_q and $f(\alpha)$ which are usually derived in the following way [see, e.g., *Macek and Wawrzaszek* 2009].

[13] Namely, for a continuous index $-\infty < q < \infty$ using a q-order total probability measure, $I(q,l) \equiv \sum_{i=1}^{N} p_i^q(l)$ with p_i as given in equation (1) and a q-order generalized information entropy $H(q,l) \equiv -\log I(q,l) = -\log \sum_{i=1}^{N} p_i^q(l)$ defined by *Grassberger and Procaccia* [1983], one obtains the usual q-order generalized dimensions [*Hentschel and Procaccia*, 1983] $D_q \equiv \tau(q) / (q-1)$, where

$$\tau(q) = \lim_{l\to 0} \frac{\left[-\log \sum_{i=1}^{N} p_i^q(l)\right]}{\log(1/l)}. \tag{2}$$

Following *Chhabra and Jensen* [1989] we also define a one-parameter q family of generalized pseudoprobability measures (normalized)

$$\mu_i(q,l) \equiv \frac{p_i^q(l)}{\sum_{i=1}^{N} p_i^q(l)}. \tag{3}$$

[14] Next, for a given q with the associated index of the fractal dimension $f_i(q,l) \equiv \log\mu_i(q,l)/\log l$ the multifractal singularity spectrum of dimensions is defined directly as the averages denoted by $\langle \ldots \rangle$ taken with respect to the measure $\mu(q,l)$ in equation (3)

$$f(q) \equiv \lim_{l\to 0} \sum_{i=1}^{N} \mu_i(q,l)\ f_i(q,l) = \langle f(q)\rangle \tag{4}$$

and the corresponding average value of the singularity strength is obtained by *Chhabra and Jensen* [1989]

$$\alpha(q) \equiv \lim_{l\to 0} \sum_{i=1}^{N} \mu_i(q,l)\ \alpha_i(l) = \langle \alpha(q)\rangle. \tag{5}$$

Hence by using a q-order mixed Shannon information entropy $S(q,l) = -\sum_{i=1}^{N} \mu_i(q,l) \log p_i(l)$ we obtain the singularity strength as a function of q

$$\alpha(q) = \lim_{l\to 0} \frac{\left[-\sum_{i=1}^{N} \mu_i(q,l) \log p_i(l)\right]}{\log(1/l)} = \lim_{l\to 0} \frac{\langle \log p_i(l)\rangle}{\log(l)}. \tag{6}$$

[15] Similarly, by using the q-order generalized Shannon entropy $K(q,l) = -\sum_{i=1}^{N} \mu_i(q,l) \log \mu_i(q,l)$ we obtain directly the singularity spectrum as a function of q

$$f(q) = \lim_{l\to 0} \frac{\left[-\sum_{i=1}^{N} \mu_i(q,l) \log \mu_i(q,l)\right]}{\log(1/l)} = \lim_{l\to 0} \frac{\langle \log \mu_i(q,l)\rangle}{\log(l)}. \tag{7}$$

One can easily verify that the multifractal singularity spectrum $f(\alpha)$ as a function of α satisfies the Legendre transformation [*Halsey et al.*, 1986]:

$$\alpha(q) = \frac{\mathrm{d}\ \tau(q)}{\mathrm{d}q}, \qquad f(\alpha) = q\alpha(q) - \tau(q). \tag{8}$$

3.3. Two-Scale Weighted Cantor Set

[16] Consider the generalized weighted Cantor set, as shown by *Macek* [2007, Figure 2], see also *Macek and Szczepaniak* [2008, Figure 1], where the probability of choosing one interval of size l_1 is p (say, $p \le 1/2$), and for the other interval of size l_2 is $1 - p$. For each step of construction of this set we use two (normalized) rescaling parameters l_1 and l_2, where $l_1 + l_2 \le L = 1$ and two (in general) different probability measures $p_1 = p$ and $p_2 = 1 - p$. In order to obtain the generalized dimensions $D_q \equiv \tau(q)/(q-1)$ for this multifractal set we use the following standard generator (also called a partition function) at the n-th step of construction [*Hentschel and Procaccia*, 1983; *Halsey et al.*, 1986]

$$\Gamma_n^q(l_1, l_2, p) = \left(\frac{p^q}{l_1^{\tau(q)}} + \frac{(1-p)^q}{l_2^{\tau(q)}}\right)^n = 1. \tag{9}$$

One sees that $\tau(q)$ does not depend on n, and after n iterations, we obtain $\binom{n}{k}$ intervals of width $l = l_1^k l_2^{n-k}$, where

$k = 1, \ldots, n$, that have quite various probabilities. The resulting set of 2^n closed intervals for $n \to \infty$ is the weighted two-scale Cantor set. We see that this multifractal set with a simple construction role exhibits a surprisingly complex structure because it consists of many more and more narrow segments of various widths and probabilities.

[17] For any q in equation (9) one obtains $D_q = \tau(q)/(q-1)$ by solving (numerically) the simple transcendental equation [e.g., *Ott*, 1993]

$$\frac{p^q}{l_1^{\tau(q)}} + \frac{(1-p)^q}{l_2^{\tau(q)}} = 1. \tag{10}$$

[18] When both scales are equal, $l_1 = l_2 = \lambda$, equation (10) can be solved explicitly to give the formula for the generalized dimensions [*Macek*, 2006, 2007]

$$\tau(q) \equiv (q-1)D_q = \frac{\ln[p^q + (1-p)^q]}{\ln\lambda}. \tag{11}$$

[19] In particular, for space filling case ($\lambda = 1/2$) one recovers the formula for the multifractal scenario of the standard p-model (e.g., for fully developed turbulence) [*Meneveau and Sreenivasan*, 1987], which obviously corresponds to the weighted one-scale Cantor set [*Hentschel and Procaccia*, 1983], [cf. *Macek*, 2002, Figure 3] and [*Macek et al.*, 2006, Figure 4].

3.4. Degree of Multifractality and Asymmetry

[20] The difference of the maximum and minimum dimension, associated with the least dense and most dense regions in the considered probability measure, is given by

$$\Delta \equiv \alpha_{\max} - \alpha_{\min} = D_{-\infty} - D_{\infty} = \left| \frac{\log(1-p)}{\log l_2} - \frac{\log(p)}{\log l_1} \right|. \tag{12}$$

In the limit $p \to 0$ this difference rises to infinity. Hence, it can be regarded as a degree of multifractality, see [e.g., *Macek*, 2006, 2007]. The degree of multifractality Δ is naturally related to the deviation from a strict self-similarity. Thus Δ is also a measure of intermittency, which is in contrast to self-similarity [*Frisch*, 1995, chapter 8]. In the case of the symmetric spectrum using equation (11) this degree of multifractality becomes

$$\Delta = D_{-\infty} - D_{+\infty} = \ln(1/p - 1)/\ln(1/\lambda). \tag{13}$$

In particular, the usual middle one-third Cantor set without any multifractality, i.e. with $\Delta = 0$, is recovered with $p = 1/2$ and $\lambda = 1/3$.

[21] Moreover, using the value of the strength of singularity α_0 at which the singularity spectrum has its maximum $f(\alpha_0) = 1$ we define a measure of asymmetry by

$$A \equiv \frac{\alpha_0 - \alpha_{\min}}{\alpha_{\max} - \alpha_0}. \tag{14}$$

Please note that the value $A = 1$ corresponds to the one-scale symmetric case (e.g., for the so-called p-model).

3.5. Multifractal Model for Magnetic Turbulence

[22] In the inertial range of the turbulence spectrum the q-order total probability measure, the partition function (using probability defined in equation (1)) should scale as

$$\sum p_j^q(l) \sim l^{\tau(q)}, \tag{15}$$

with $\tau(q)$ given in equation (2). In this case, *Burlaga* [1995] has shown that the average value of the qth moment of the magnetic field strength B at various scales $l = v_{sw}\Delta t$ scales as

$$\langle B^q(l) \rangle \sim l^{\gamma(q)}, \tag{16}$$

with the similar exponent $\gamma(q) = (q-1)(D_q - 1)$.

4. Results

[23] As usual we have analyzed the slopes $\gamma(q)$ of $\log_{10}\langle B^q \rangle$ versus $\log_{10} l$ and identified the range of scales from 2 to 16 days, over which the multifractal spectra are applicable. This has allowed us to obtain the values of D_q as a function of q according to equation (2). Equivalently, as discussed in section 3.2, the multifractal spectrum $f(\alpha)$ as given by equation (7) as a function of scaling indices α, see equation (6), exhibits universal properties of multifractal scaling behavior. Please note that we do not need to use Legendre transformation of equation (8), since the multifractal spectrum can be more reliably calculated directly from the slopes of the suitable generalized probabilities on the logarithmic scales.

4.1. Multifractal Spectra for Voyager 2 Data

[24] In this paper the results for the singularity multifractal spectrum $f(\alpha)$ obtained using the Voyager 2 data of the solar wind magnetic fields are presented in a wide range of distances in the whole heliosphere. Namely the calculated spectra in the relatively near heliosphere at 6–47 AU (1980–1995), i.e. basically within the planetary orbits, and in the distant heliosphere beyond the planets at 57–81 AU (1999–2006) are shown in Figures 3 and 4, correspondingly.

[25] The error bars resulting from the uncertainties of determining the corresponding slopes are only given here. Naturally, we are aware that the errors in magnetic field measurements itself could possibly influence the calculated spectra. Actually, after 1990, the angles of the field measured by Voyager 2 are rather uncertain and the magnetic field strength has been contaminated by large aperiodic oscillations owing to telemetry system (at least half of the time on the range ~2–10 hours), which could affect the data for hour averages [*Burlaga and Ness*, 1994; *Burlaga et al.*, 2002]. One can however hope that this effect is somewhat smaller on daily averages used in our study. For example, the data in Figure 3a and 3b, before 1990, are relatively free of the artificial amplitude fluctuations of magnetic fields, but the errors in determining the slopes are rather large. On the contrary, the data for 1990 in Figure 3c show that the slope error is small (e.g., for the last point at $\alpha = 1.12 \pm 0.008$ we have $f = 0.83 \pm 0.015$). However, since the possible spurious large-scale fluctuations of the field, as large as $\sim\pm 0.04$nT [*Burlaga and Ness*, 1994], could be contributing to the multifractal spectrum, we have taken this into account by calculating the effective error bars that should not be larger than by about factor of 2 (in this case for $\alpha = 1.14 \pm 0.02$ we have $f = 0.84 \pm 0.025$). In spite of this error in magnetic field

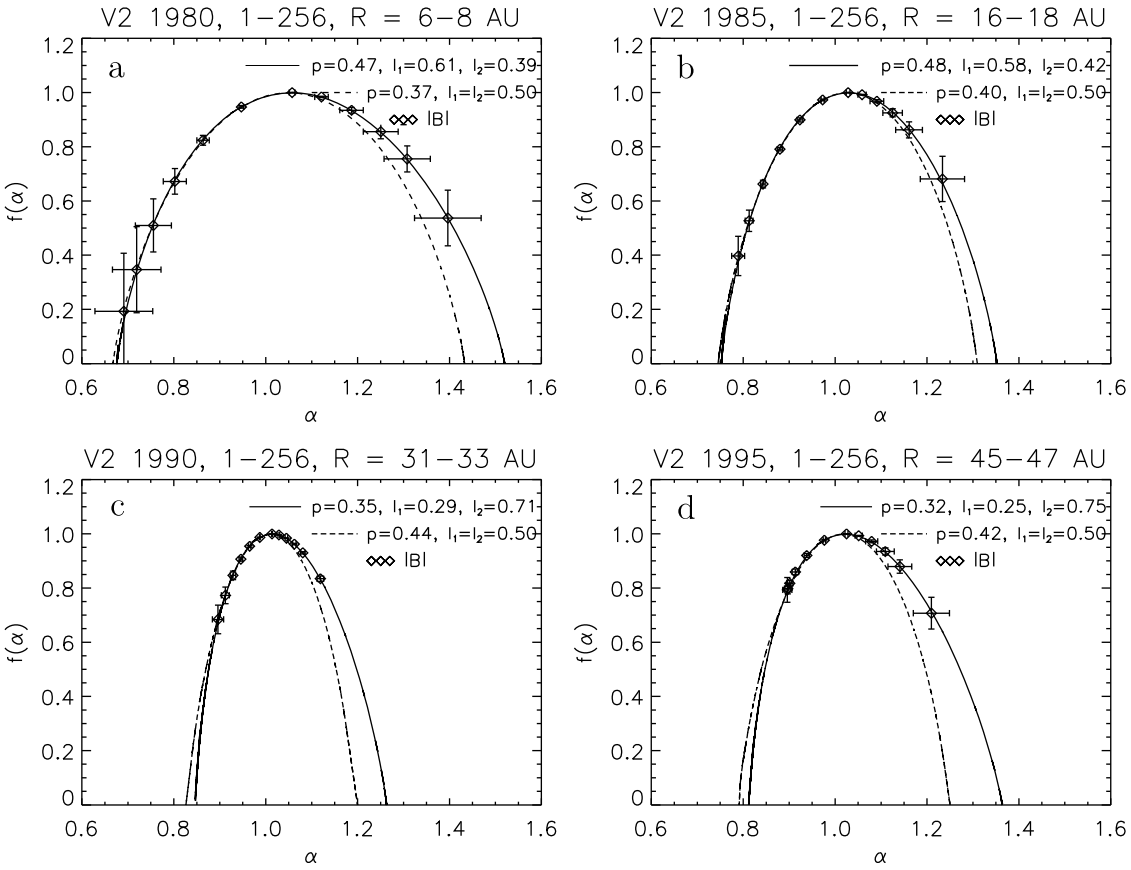

Figure 3. The singularity spectrum $f(\alpha)$ as a function of a singularity strength α. The values are calculated for the weighted two-scale (continuous lines) model and the usual one-scale (dashed lines) p-model with the parameters fitted using the magnetic fields (diamonds) measured by Voyager 2 in the near heliosphere at (a) 6–8 AU, (b) 16–18 AU, (c) 31–33 AU, and (d) 45–47 AU, correspondingly.

measurements we have verified that the calculated spectrum still remains asymmetric. Admittedly, even with the slope error bars it is sometimes difficult to distinguish between symmetric spectrum and an asymmetric spectrum, e.g., only one or two points in Figure 3 determine the asymmetry.

[26] Again, during the period of 1999–2006 shown in Figure 4 spurious large amplitude fluctuations in magnetic field are still present and the average magnetic field strength is very weak, close to the measurement uncertainties. There is a difference in the symmetric and asymmetric spectra only for the 2003 data, Figure 4b, and only one point determines asymmetry. Moreover, the results for the heliosheath, i.e. after crossing the heliospheric shock by Voyager 1 (at 94 AU) in 2004, are presented in Figure 5a at 94–97 AU for the year 2005 and Figure 5c at 105–107 AU for the year 2008. Similarly, the results for Voyager 2, which crossed the shock at 84 AU in 2007, are presented in Figure 5b at 85–88 AU for the year 2008 and Figure 5d at 88–90 AU for the year 2009, correspondingly. Here also it is difficult to argue that there is an asymmetry in these spectra for the Voyager 1 data, but there is some deviation from symmetric spectrum for Voyager 2.

[27] Next, we are looking for the degree of multifractality Δ in the heliosphere, as given in equation (12), as a function of the heliospheric distances during four time intervals, namely during solar minimum (MIN), solar maximum (MAX), declining (DEC) and rising (RIS) phases of solar cycles as shown in Figure 6. We see that the obtained values of Δ for Voyager 2 roughly follow the fitted function of time (in years, x), $0.44 + 0.10\exp(-(x-10)/50) + 0.25\exp(-(x-10)/30)\cos(2\pi/(40-0.15x)(x-10))$, shown by a continuous line, which is periodic and decreasing with the distance from the Sun. In particular, the value for 25 AU is consistent with that obtained by *Burlaga* [1991]. The crossing of the termination shock (TS) by Voyager 2 at 84 AU is marked by a vertical dashed line. Below are shown the Sunspot Numbers (SSN) during the period of years 1980–2009. This is worth noting that the degree of multifractality measured by Voyager 2 appears to vary with solar activity. We claim that in spite of the uncertainty in the measurements, it is a real effect. This is probably because the large merged interaction regions and global merged interaction regions occurring near solar maximum have very large magnetic field strengths and fluctuations, which dominate the uncertainties.

[28] In addition, the degree of asymmetry A of the multifractal spectrum defined by equation (14) calculated in the heliosphere as a function of the heliocentric distances for Voyager 2 is shown in Figure 7. Please note that the value $A = 1$ (dashed) corresponds to the one-scale symmetric model. It appears that the value of the degree of asymmetry

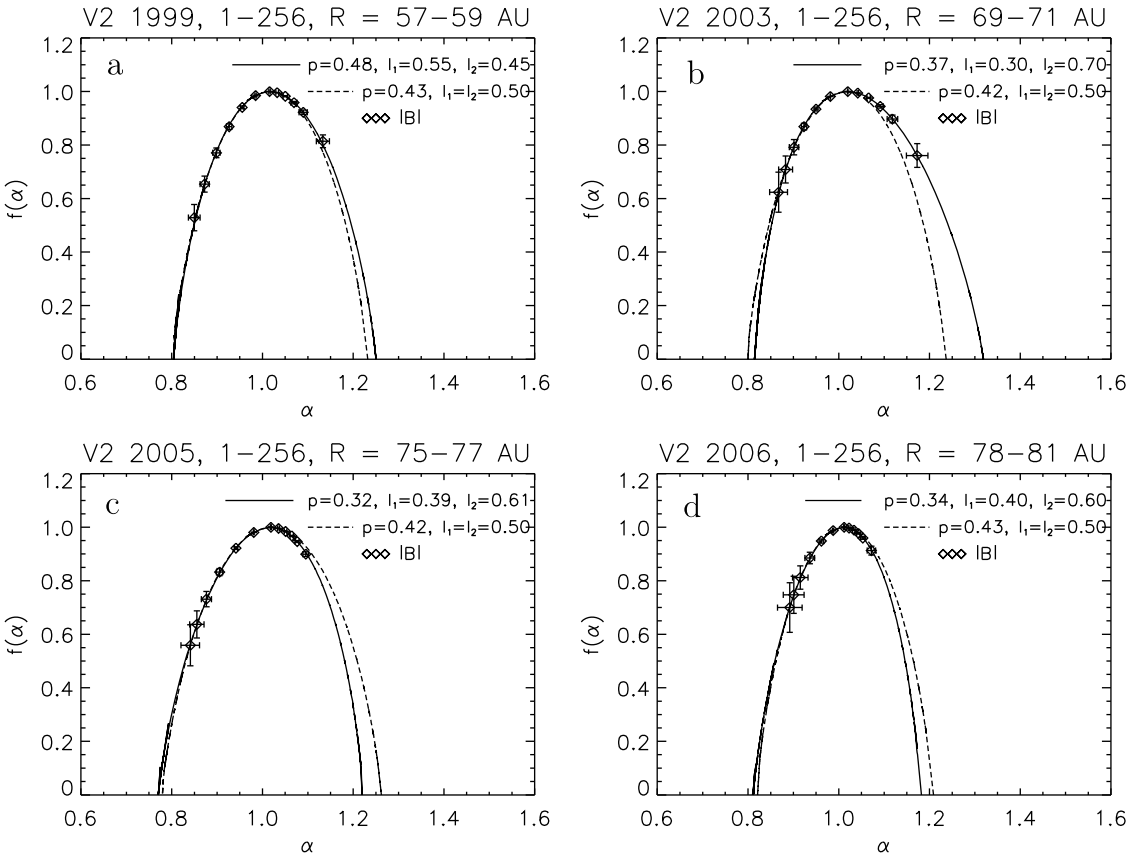

Figure 4. The singularity spectrum $f(\alpha)$ as a function of a singularity strength α. The values are calculated for the weighted two-scale (continuous lines) model and the usual one-scale (dashed lines) *p*-model with the parameters fitted using the magnetic fields (diamonds) measured by Voyager 2 in the distant heliosphere at various distances before crossing the termination shock, (a) 57–59 AU, (b) 69–71 AU, (c) 75–77 AU, and (d) 78–81 AU, correspondingly.

A decreases (in other words the spectrum becomes more asymmetric) with increasing distance between 5 AU and 50 AU. This is very possible, since merged interaction regions, which could be ultimately responsible for the asymmetry, form and develop in this region [*Burlaga et al.*, 2003]. However, Figure 7 suggests that the degree of asymmetry is roughly constant ($A \sim 1$, symmetric spectrum) between 50 AU and the termination shock. This is plausible, because the merged interaction regions damp out here, as discussed by *Burlaga et al.* [2007].

[29] We see that similarly as for Voyager 1 in the heliosphere there could only be few points above unity at large heliospheric distances [cf. *Macek et al.*, 2011]. Really, inside the distant heliosphere prevalently $A < 1$ and only twice (during the declining phase) the left-skewed spectrum ($A > 1$) was possibly observed, even though it is still consistent with a symmetric spectrum. Anyhow, we see that the right-skewed spectrum ($A < 1$) before the crossing of the termination shock is preferred for both Voyager 1 and 2 data. Again the multifractal scaling is asymmetric before shock crossing with the calculated degree of asymmetry at distances 60–80 AU equal to $A = 0.74$–1.14.

[30] We can also verify that the asymmetry is possibly changing when crossing the termination shock ($A = 0.66$–0.83 for distances of 85–90 AU), as is also seen in Figure 7 (cf. Figures 4d and 5b), but because of large errors bars and a rather limited sample, symmetric spectrum is still possible beyond the termination shock [cf. *Burlaga and Ness*, 2010]. It is hence worth noting a possible change of the symmetry of the spectrum at the shock relative to its maximum at a critical singularity strength $\alpha = 1$. Because the density of the measure $\varepsilon \propto l^{\alpha-1}$, this is in fact related to changing properties of the magnetic field density ε at the termination shock.

4.2. Comparison With Voyager 1

[31] We have already seen from Figures 5a and 5c and Figures 5b and 5d that the multifractal spectra for both Voyager 1 and 2 are basically similar. However, between launch in 1977 and 1990, the problem of artificial magnetic field fluctuations was increasingly significant. In fact, the uncertainties associated with the Voyager 2 data are often larger than those associated with the Voyager 1 data [*Burlaga and Ness*, 1994]. Therefore, it is interesting that multifractal spectra derived from the Voyager 2 data resemble those derived from the Voyager 1 data.

[32] Moreover, these values of Δ are apparently modulated by the solar activity, depending on a specific solar cycle, as shown in Figure 6 for the case of Voyager 2, as already noted by *Burlaga et al.* [2003]. Now, referring to *Macek et al.* [2011, Figure 2], Figure 8 shows that the degree of multifractality for both Voyager 1 and 2 decreases with

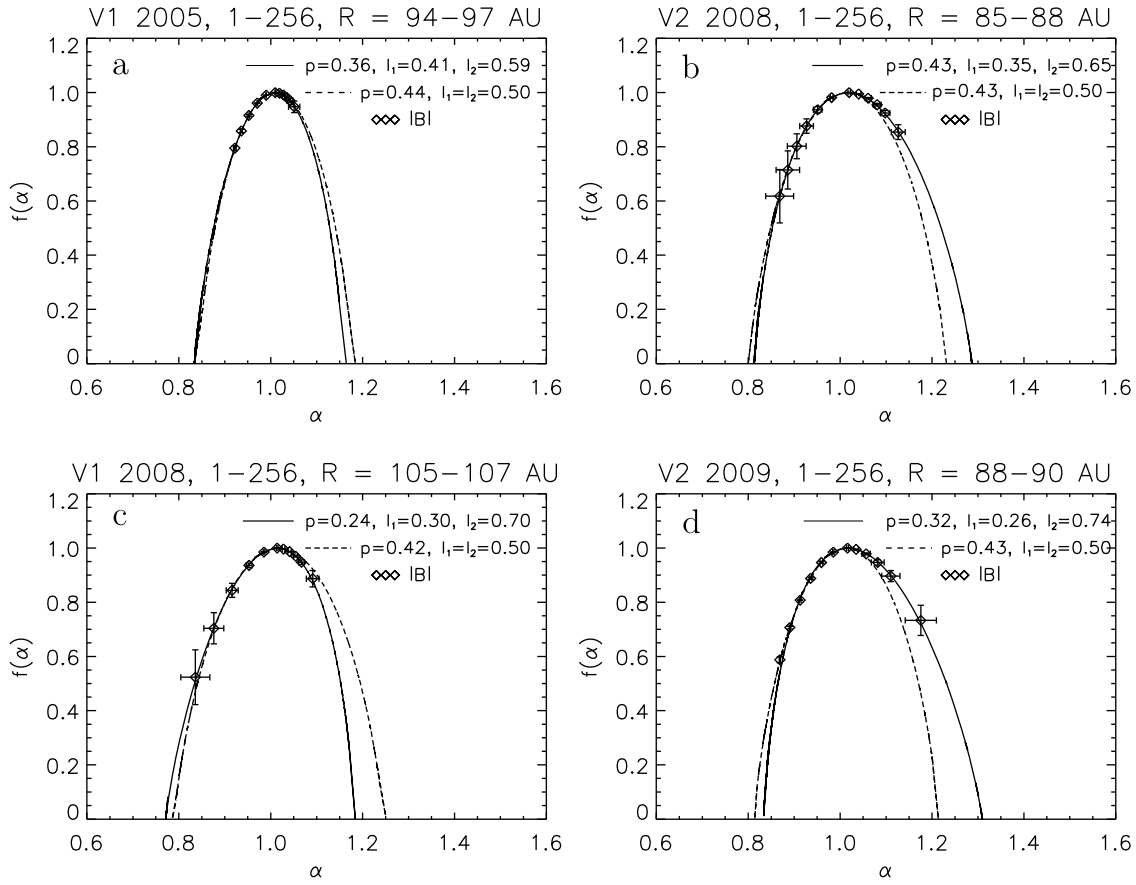

Figure 5. The singularity spectrum $f(\alpha)$ as a function of a singularity strength α. The values are calculated for the weighted two-scale (continuous lines) model and the usual one-scale (dashed lines) p-model with the parameters fitted using the magnetic fields (diamonds) measured by Voyager 1 in the heliosheath at various heliocentric distances of (a) 94–97 AU and (c) 105–107 AU, and Voyager 2 at (b) 85–88 AU and (d) 88–90 AU, correspondingly.

increasing distance from the Sun [cf. *Burlaga et al.*, 2003, 2007]. We can verify that the degree of multifractality for both spacecraft falls steadily with distance, following roughly linear fits of $-0.0028\ x + 0.6769$ and $-0.0024\ x + 0.6292$ for Voyager 1 and 2, correspondingly (with the errors in the slope of the fits 0.0006 and 0.0009; the correlation coefficient is 0.37). Again, it is remarkable that the Voyager 2 and Voyager 1 data give similar results, given the systematic uncertainties in the Voyager 2 data at large distances.

[33] The degree of asymmetry A of the multifractal spectrum in the heliosphere as a function of the heliocentric distances for both Voyager 1 and 2 data is shown in Figure 9. The crossings of the termination shock (TS) by Voyager 1 and 2 are marked by vertical dashed lines. We see an apparent increase in the deviation from symmetric spectrum with increasing distance between 5 and 50 AU observed by Voyager 1 and Voyager 2 and relatively symmetric spectra between 50 AU and termination shock. These results are consistent with the growth and evolution and decay of interaction regions described and modeled by *Burlaga et al.* [2007].

[34] In case of Voyager 1 (Figure 9), we have already seen that in contrast to the right-skewed asymmetric spectrum with singularity strength $\alpha > 1$ ($A < 1$) inside the heliosphere, the spectrum becomes more left-skewed in the heliosheath, $\alpha < 1$ ($A > 1$) [*Macek et al.*, 2011]. Consequently, a concentration of magnetic fields should shrink resulting in thinner flux tubes or stronger current concentration in the heliosheath, see [e.g., *Borovsky*, 2008]. Similarly, localized merging of coherent magnetic structures has been proposed for the magnetotail by *Wu and Chang* [2000] and for the heliospheric turbulence by *Bruno et al.* [2001].

[35] Now, in the case of Voyager 2 we see in Figures 7 and 9 that this tendency is somehow reversed. But still we observe a change of the asymmetry of the spectrum when crossing the termination shock. Admittedly, we can also have approximately symmetric spectrum in the heliosheath, where the plasma is expected to be roughly in equilibrium in the transition to the interstellar medium. At this point it is worth noting that magnetic fields in the heliosheath were normally distributed (Voyager 1) in contrast to the lognormal distribution in the outer heliosphere [*Burlaga et al.*, 2005], while distributions observed by Voyager 2 were approximately lognormal both before the shock crossing and in the heliosheath [*Burlaga et al.*, 2009]. *Chen et al.* [2008] has proposed a mechanism to demonstrate that the strength of magnetic field can be transformed from a lognormal to

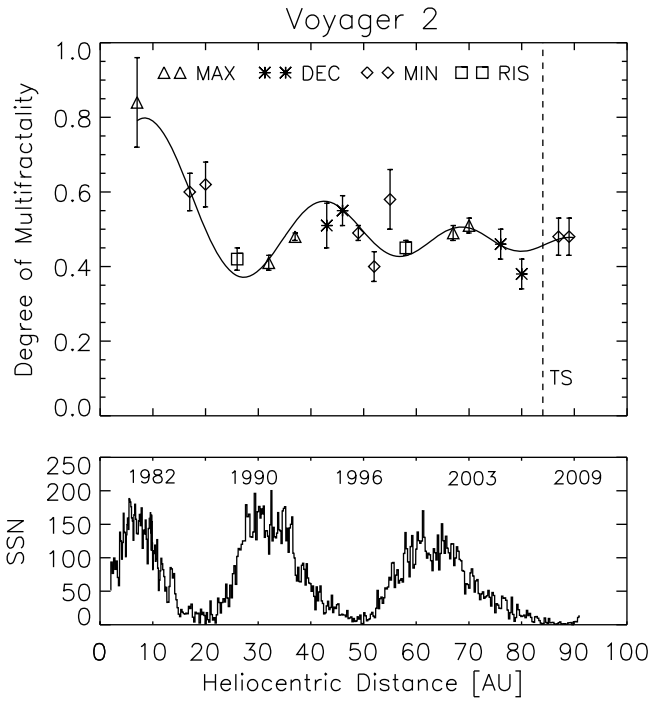

Figure 6. (top) The degree of multifractality Δ in the heliosphere as a function of the distances from the Sun fitted to a periodically decreasing function shown by a continuous line during solar minimum (MIN) and solar maximum (MAX), declining (DEC) and rising (RIS) phases of solar cycles. The crossing of the termination shock by Voyager 2 is marked by a vertical dashed line (TS). (bottom) Sunspot Numbers (SSN) during the period of 1980–2009.

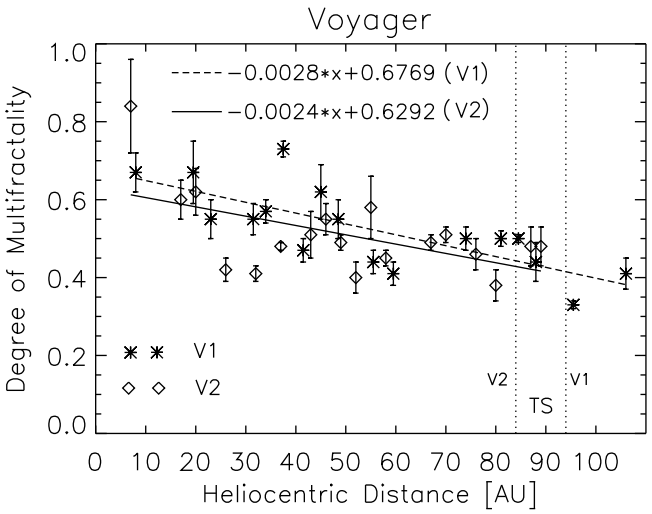

Figure 8. The degree of multifractality Δ in the heliosphere versus the heliospheric distances for Voyager 1 and 2 with fits to straight lines. The crossings of the termination shock (TS) by both spacecraft are marked by vertical dotted lines.

a normal distribution provided that small β plasma (say, of $\sim$0.1) is present near the termination shock; for β higher (of $\sim$10) the distribution should remain lognormal. This would explain the Voyager 1 data [*Burlaga et al.*, 2005], and not necessarily all Voyager 2 observations. In the later case a low-β plasma has been observed just before shock crossing, but the distributions were approximately lognormal in both solar wind and magnetosheath, where the variations of the magnetic field were neither stationary nor homogeneous [cf. *Burlaga et al.*, 2009]. Presumably, a reformation of the local complex structure of the shock

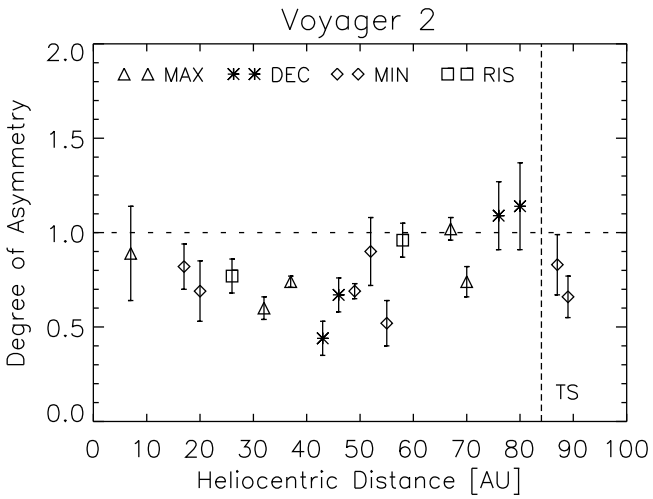

Figure 7. The degree of asymmetry A of the multifractal spectrum in the heliosphere as a function of the heliospheric distances during solar minimum (MIN) and solar maximum (MAX), declining (DEC) and rising (RIS) phases of solar cycles. The value $A = 1$ corresponds to the one-scale symmetric model (dashed). The crossing of the termination shock by Voyager 2 is marked by a vertical (dashed) line, TS.

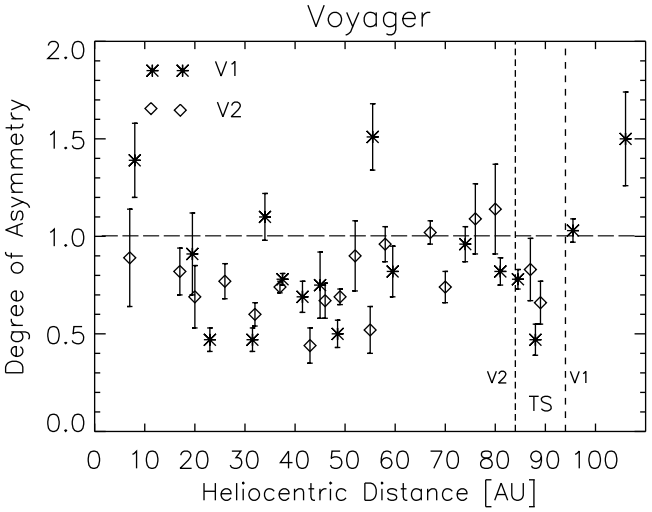

Figure 9. The degree of asymmetry A of the multifractal spectrum in the heliosphere as a function of the heliospheric distance; the value $A = 1$ (dashed) corresponds to the one-scale symmetric model. The crossings of the termination shock (TS) by Voyager 1 and 2 are marked by vertical dotted lines.

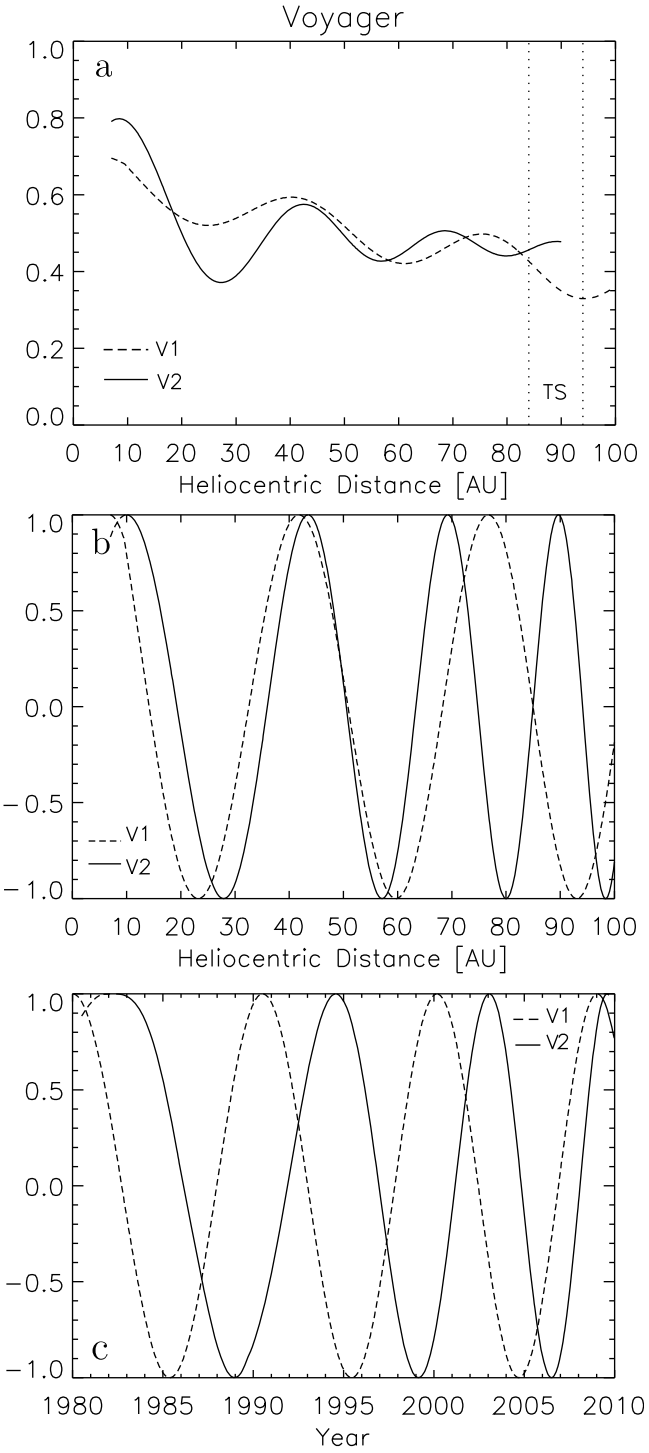

Figure 10. (a) Comparison of the functions fitted to the obtained degree of multifractality versus heliocentric distances for Voyager 1 (dashed line) and 2 (continuous line; cf. Figure 6). The periodic parts of functions depending on (b) heliocentric distances and (c) time.

and the influence of ionized interstellar atoms have to be also taken into consideration [*Burlaga et al.*, 2008].

[36] In addition, the periodic parts (without taking into account amplitudes) for the functions used to fit the calculated degrees of multifractality, as shown in Figure 10a (cf. Figure 6) are now presented in Figures 10b and 10c as functions of heliocentric distances and time, correspondingly, for both Voyager 1 (dashed lines) and Voyager 2 (continuous lines). One can notice that the degrees of multifractality observed by both spacecraft especially in the outer heliosphere beyond the planetary orbits (say, for distances greater than 50 AU) are shifted by distances of about 10 AU (Figure 10b) or delayed by several years (Figure 10c). Therefore, it would be interesting to look for a possible mechanism responsible for such a correlation, which also results in the normal or lognormal distribution of the observed magnetic fields, e.g., as proposed by *Chen et al.* [2008].

[37] Please note that while Voyager 1 is located in the northward solar hemisphere, Voyager 2 is exploring southward hemisphere, Figure 1. Naturally, the latitudinal variations of Voyager 1 and 2 should be taken into consideration. In fact, moving toward higher latitudes implies sampling more and more fast and steady solar wind. As a consequence, we would expect that the degree of intermittency Δ should decrease at higher latitudes since the fast wind is less intermittent than the slow wind [*Bruno et al.*, 2003; *Wawrzaszek and Macek*, 2010]. This effect might possibly contribute to the general decreasing trend observed in Figures 6 and 8. On the other hand, the modulation observed in Figure 6 might also be related to the fast wind at low latitudes. In particular, the first decrease of Δ in Figure 6 is probably because Voyager 2 starts to sample more and more the fast wind in the ecliptic owing to the decreasing phase of the solar cycle. Moreover, Voyager 1 would start to see the first decrease of the degree of multifractality before Voyager 2 because it is located at higher latitudes. This could also be reflected on the fact that Voyager 1 reaches its first minimum value of Δ before Voyager 2 in Figure 10a. In this way, one can therefore hope to infer from the time delay some information about the evolution of the whole heliosphere.

[38] Finally, Table 1 summarizes the values of Δ and A calculated for Voyager 2 data in the relatively near heliosphere (within the planetary system, up to 40 AU; cf. Figure 3), the outer heliosphere (i.e., beyond the planets), and the distant heliosphere (60–80 AU; Figure 4), together with those in the heliosheath (85–90 AU; Figures 5b and 5d). For comparison, the values calculated for Voyager 1 together with the corresponding values obtained from the papers by *Burlaga et al.* [2006] and *Burlaga and Ness* [2010] (LB) have also been given in *Macek et al.* [2011, Table 1] (cf. Figures 5a and 5c). Also a particular value of the degree of multifractality at 25 AU (Figure 6) is in agreement with the value obtained by *Burlaga* [1991]. It is hence worth noting that the multifractal characteristics for fluctuations of the interplanetary magnetic field strength obtained from independent types of studies are in surprisingly good agreement.

[39] Generally, these values for Voyager 2 are also smaller than that for the energy rate transfer in the turbulence cascade (Δ = 2–3) [*Macek and Wawrzaszek*, 2009]. Moreover, it is worth noting that our values obtained before the shock crossing, Δ = 0.4–0.5, are similar to those for the heliosheath Δ = 0.5. We have obtained roughly constant values of Δ in the heliosheath, which is consistent with a metastable

Table 1. The Degree of Multifractality Δ and Asymmetry A of the Multifractal Spectrum for the Magnetic Field Strength Observed by Voyager 2 at Various Heliocentric Distances, Before and After Crossing the Termination Shock

Heliocentric Distance	Years	Multifractality Δ	Asymmetry A
7–40 AU	1980–1990	0.41–0.85	0.61–0.90
40–60 AU	1992–1999	0.40–0.58	0.44–0.96
60–80 AU	2002–2006	0.38–0.50	0.74–1.14
85–90 AU	2008–2009	0.47–0.48	0.66–0.83

equilibrium, as suggested by *Burlaga and Ness* [2010] for the case of Voyager 1.

5. Conclusions

[40] Basically, in this paper we show that for both Voyager 1 and 2, located above and below the solar equatorial plane, respectively, the degree of multifractality for magnetic field fluctuations of the solar wind falls steadily with the distance from the Sun. But now it seems that this quantity is modulated by the solar activity with a time delay of several years, corresponding to a difference of distances of about 10 AU in the very distant heliosphere. That would certainly require a specific mechanism responsible for such a correlation, resulting in the normal or lognormal distribution of the observed magnetic fields. This in turn can hopefully allows us to infer some new important information about the nature of the heliospheric shock and also about the evolution of the whole heliosphere.

[41] We have again observed a change of the asymmetry of the spectrum when crossing the termination shock by Voyager 1 and 2. Consequently, a concentration of magnetic fields shrinks (stretches) resulting in thinner (fatter) flux tubes or stronger (weaker) current concentration in the heliosheath. Admittedly, we can still have approximately symmetric spectrum in the heliosheath, where the plasma is expected to be roughly in equilibrium in the transition to the interstellar medium. In particular, we also confirm our earlier results that before the shock crossing, especially during solar maximum, turbulence is more multifractal than that in the heliosheath [*Macek et al.*, 2011]. We are however aware that the multifractal quantities could be possibly influenced by the interactions among shocks and large-scale features that are produced by dynamical processes, which are quite distinct from turbulence.

[42] In addition, in the whole heliosphere during solar minimum the spectrum is dominated by values of $\alpha > 1$, which could change when crossing the termination heliospheric shock. This may represents a first direct in situ information of interest in the astrophysical context. In fact, a density of measure dominated by $\alpha < 1$ ($\alpha > 1$) would imply that the magnetic field in the very local interstellar medium is roughly confined in thin (thick) filaments of high (low) magnetic density. That means that it would be interesting to investigate whether the heliosheath is dominated by 'voids' of magnetic fields in the very local interstellar medium related to the presence of very localized intense magnetic field structures. Such information, obtained in situ and not only remotely (through scintillations observations), are important in the context of question of interstellar turbulence and stellar formation modeling [e.g., *Spangler*, 2009]. Finally, it is worth mentioning that our analysis brings significant additional support to earlier results suggesting that the solar wind termination shock is asymmetric [*Stone et al.*, 2008].

[43] **Acknowledgments.** This work has been supported by the Polish National Science Centre (NCN) and the Ministry of Science and Higher Education (MNiSW) through grant NN 307 0564 40. We would like to thank the magnetic field instruments team of Voyager mission, the NASA National Space Science Data Center and the Space Science Data Facility for providing Voyager 1 and 2 data. We thank referees for drawing our attention to the data uncertainties and for their kind help in interpretation of our results.

[44] Philippa Browning thanks the reviewers for their assistance in evaluating this paper.

References

Borovsky, J. E. (2008), Flux tube texture of the solar wind: Strands of the magnetic carpet at 1 AU?, *J. Geophys. Res.*, *113*, A08110, doi:10.1029/2007JA012684.

Bruno, R., and V. Carbone (2005), The solar wind as a turbulence laboratory, *Living Rev. Sol. Phys.*, *2*, 4.

Bruno, R., V. Carbone, P. Veltri, E. Pietropaolo, and B. Bavassano (2001), Identifying intermittency events in the solar wind, *Planet. Space Sci.*, *49*, 1201–1210.

Bruno, R., V. Carbone, L. Sorriso-Valvo, and B. Bavassano (2003), Radial evolution of solar wind intermittency in the inner heliosphere, *J. Geophys. Res.*, *108*(A3), 1130, doi:10.1029/2002JA009615.

Burlaga, L. F. (1991), Multifractal structure of the interplanetary magnetic field: Voyager 2 observations near 25 AU, 1987–1988, *Geophys. Res. Lett.*, *18*, 69–72.

Burlaga, L. F. (1995), *Interplanetary Magnetohydrodynamics*, Oxford Univ. Press, New York.

Burlaga, L. F. (2001), Lognormal and multifractal distributions of the heliospheric magnetic field, *J. Geophys. Res.*, *106*, 15,917–15,927, doi:10.1029/2000JA000107.

Burlaga, L. F. (2004), Multifractal structure of the large-scale heliospheric magnetic field strength fluctuations near 85 AU, *Nonlinear Processes Geophys.*, *11*, 441–445.

Burlaga, L. F., and N. F. Ness (1994), Merged interaction regions and large-scale magnetic field fluctuations during 1991: Voyager 2 observations, *J. Geophys. Res.*, *99*, 19,341–19,350, doi:10.1029/94JA01513.

Burlaga, L. F., and N. F. Ness (2010), Sectors and large-scale magnetic field strength fluctuations in the heliosheath near 110 AU: Voyager 1, 2009, *Astrophys. J.*, *725*, 1306–1316, doi:10.1088/0004-637X/725/1/1306.

Burlaga, L. F., N. F. Ness, Y.-M. Wang, and N. R. Sheeley (2002), Heliospheric magnetic field strength and polarity from 1 to 81 AU during the ascending phase of solar cycle 23, *J. Geophys. Res.*, *107*(A11), 1410, doi:10.1029/2001JA009217.

Burlaga, L. F., C. Wang, and N. F. Ness (2003), A model and observations of the multifractal spectrum of the heliospheric magnetic field strength fluctuations near 40 AU, *Geophys. Res. Lett.*, *30*(10), 1543, doi:10.1029/2003GL016903.

Burlaga, L. F., N. F. Ness, M. H. Acuña, R. P. Lepping, J. E. P. Connerney, E. C. Stone, and F. B. McDonald (2005), Crossing the termination shock into the heliosheath: Magnetic fields, *Science*, *309*, 2027–2029, doi:10.1126/science.1117542.

Burlaga, L. F., N. F. Ness, and M. H. Acuña (2006), Multiscale structure of magnetic fields in the heliosheath, *J. Geophys. Res.*, *111*, A09112, doi:10.1029/2006JA011850.

Burlaga, L. F., A. F-Viñas, and C. Wang (2007), Tsallis distributions of magnetic field strength variations in the heliosphere: 5 to 90 AU, *J. Geophys. Res.*, *112*, A07206, doi:10.1029/2006JA012213.

Burlaga, L. F., N. F. Ness, M. H. Acuña, R. P. Lepping, J. E. P. Connerney, and J. D. Richardson (2008), Magnetic fields at the solar wind termination shock, *Nature*, *454*, 75–77, doi:10.1038/nature07029.

Burlaga, L. F., N. F. Ness, M. H. Acuña, J. D. Richardson, E. Stone, and F. B. McDonald (2009), Observations of the heliosheath and solar wind near the termination shock by Voyager 2, *Astrophys. J.*, *692*, 1125–1130, doi:10.1088/0004-637X/692/2/1125.

Burlaga, L. F., N. F. Ness, Y.-M. Wang, N. R. Sheeley, and J. D. Richardson (2010), Observations of the magnetic field and plasma in the heliosheath by Voyager 2 from 2007.7 to 2009.4, *J. Geophys. Res.*, *115*, A08107, doi:10.1029/2009JA015239.

Carbone, V. (1993), Cascade model for intermittency in fully developed magnetohydrodynamic turbulence, *Phys. Rev. Lett.*, *71*, 1546–1548, doi:10.1103/PhysRevLett.71.1546.

Chen, M. Q., J. K. Chao, L. C. Lee, and N. H. Ting (2008), Heliosphere termination shock as a transformer of magnetic field from lognormal to normal distribution, *Astrophys. J.*, *680*, L145–L148, doi:10.1086/589569.

Chhabra, A., and R. V. Jensen (1989), Direct determination of the f(α) singularity spectrum, *Phys. Rev. Lett.*, *62*(12), 1327–1330, doi:10.1103/PhysRevLett.62.1327.

Frisch, U. (1995), *Turbulence: The legacy of A.N. Kolmogorov*, Cambridge Univ. Press, Cambridge, U. K.

Grassberger, P., and I. Procaccia (1983), Measuring the strangeness of strange attractors, *Physica D*, *9*, 189–208, doi:10.1016/0167-2789(83)90298-1.

Halsey, T. C., M. H. Jensen, L. P. Kadanoff, I. Procaccia, and B. I. Shraiman (1986), Fractal measures and their singularities: The characterization of strange sets, *Phys. Rev. A*, *33*, 1141–1151, doi:10.1103/PhysRevA.33.1141.

Hentschel, H. G. E., and I. Procaccia (1983), The infinite number of generalized dimensions of fractals and strange attractors, *Physica D*, *8*, 435–444, doi:10.1016/0167-2789(83)90235-X.

Kolmogorov, A. (1941), The local structure of turbulence in incompressible viscous fluid for very large Reynolds' numbers, *Dokl. Akad. Nauk SSSR*, *30*, 301–305.

Kraichnan, R. H. (1965), Inertial-range spectrum of hydromagnetic turbulence, *Phys. Fluids*, *8*, 1385–1387.

Macek, W. M. (1998), Large-scale structure and termination of the heliosphere, in *Highlights of Astronomy*, vol. 11B, p. 851–856, Kluwer Acad., Dordrecht, Netherlands.

Macek, W. M. (2002), Multifractality and chaos in the solar wind, *AIP Conf. Proc.*, *622*, 74–79, doi:10.1063/1.1487522.

Macek, W. M. (2006), Modeling multifractality of the solar wind, *Space Sci. Rev.*, *122*, 329–337, doi:10.1007/s11214-006-8185-z.

Macek, W. M. (2007), Multifractality and intermittency in the solar wind, *Nonlinear Processes Geophys.*, *14*, 695–700.

Macek, W. M., and A. Szczepaniak (2008), Generalized two-scale weighted Cantor set model for solar wind turbulence, *Geophys. Res. Lett.*, *35*, L02108, doi:10.1029/2007GL032263.

Macek, W. M., and A. Wawrzaszek (2009), Evolution of asymmetric multifractal scaling of solar wind turbulence in the outer heliosphere, *J. Geophys. Res.*, *114*, A03108, doi:10.1029/2008JA013795.

Macek, W. M., R. Bruno, and G. Consolini (2006), Testing for multifractality of the slow solar wind, *Adv. Space Res.*, *37*, 461–466, doi:10.1016/j.asr.2005.06.057.

Macek, W. M., A. Wawrzaszek, and V. Carbone (2011), Observation of the multifractal spectrum at the termination shock by Voyager 1, *Geophys. Res. Lett.*, *38*, L19103, doi:10.1029/2011GL049261.

Meneveau, C., and K. R. Sreenivasan (1987), Simple multifractal cascade model for fully developed turbulence, *Phys. Rev. Lett.*, *59*, 1424–1427, doi:10.1103/PhysRevLett.59.1424.

Ott, E. (1993), *Chaos in Dynamical Systems*, Cambridge Univ. Press, Cambridge, U. K.

Richardson, J. D., C. Wang, and L. F. Burlaga (2004), The solar wind in the outer heliosphere, *Adv. Space Res.*, *34*, 150–156, doi:10.1016/j.asr.2003.03.066.

Spangler, S. R. (2009), Plasma turbulence in the Local Bubble, *Space Sci. Rev.*, *143*, 277–290, doi:10.1007/s11214-008-9391-7.

Stone, E. C., A. C. Cummings, F. B. McDonald, B. C. Heikkila, N. Lal, and W. R. Webber (2008), An asymmetric solar wind termination shock, *Nature*, *454*, 71–74, doi:10.1038/nature07022.

Szczepaniak, A., and W. M. Macek (2008), Asymmetric multifractal model for solar wind intermittent turbulence, *Nonlinear Processes Geophys.*, *15*, 615–620.

Wawrzaszek, A., and W. M. Macek (2010), Observation of the multifractal spectrum in solar wind turbulence by Ulysses at high latitudes, *J. Geophys. Res.*, *115*, A07104, doi:10.1029/2009JA015176.

Wu, C. C., and T. Chang (2000), 2D MHD simulation of the emergence and merging of coherent structures, *Geophys. Res. Lett.*, *27*(6), 863–866, doi:10.1029/1999GL003704.